

DWC Hydroponic roofs for building decarbonization: a parametric dynamic thermal analysis

Francesco Nocera^{1*}, Vincenzo Costanzo², Maurizio Detommaso¹, Gianpiero Evola², Sonia Longo³, and Marina Mistretta⁴

¹Department of Civil Engineering and Architecture, University of Catania, Catania, Italy

²Department of Electric, Electronics, and Computer Engineering, University of Catania, Catania, Italy

³Department of Engineering, University of Palermo, Palermo, Italy

⁴Department of Information Engineering, Infrastructure and Sustainable Energy, University Mediterranea of Reggio Calabria, Reggio Calabria, Italy

Abstract. This study investigates the potential of a modular Deep Water Culture (DWC) hydroponic roof as a passive strategy for building decarbonization and energy demand reduction. The proposed system represents an alternative to conventional green roofs, combining the thermal inertia provided by a water layer with the principles of Building-Integrated Architecture (BIA). A parametric dynamic thermal analysis was carried out to evaluate the influence of the hydroponic water depth on the energy and thermal performance of buildings. To this aim a validated TRNSYS model, calibrated against on-site experimental measurements was used. Three different water depths in the hydroponic tray (20 cm, 30 cm, and 40 cm) were analysed in combination with three roof typologies: an uninsulated reinforced concrete slab with hollow clay blocks, an insulated concrete roof and a lightweight prefabricated roof. Seasonal heating and cooling energy demands, surface temperatures, time lag and decrement factor were investigated. The results demonstrate that a water depth of 20 cm represents the optimal configuration across all roof typologies leading to a reduction in cooling energy demand of up to 45%, an increase in time lag from 7 h to 14 h and a decrease in peak external surface temperature exceeding 10 °C during summer. Increasing the water depth beyond 20 cm does not provide additional benefits and may even degrade summer performance due to excessive thermal resistance and heat storage effects. The most significant improvements were observed for lightweight roofs, which inherently lack thermal inertia.

Keywords: Hydroponic roofs, Deep Water Culture (DWC), dynamic thermal performance, building energy demand, thermal inertia.

* Corresponding author: francesconocera@unict.it

1 Introduction

The reduction of carbon dioxide emissions due to high energy consumption in buildings represents one of the greatest environmental issues [1]. In the last decades, the urban expansion processes, the notable usage of materials with high solar absorptivity, and the reduction of vegetated areas have favoured the increase in the outdoor air temperature in the urban areas [2, 3]. More severe urban microclimate conditions have led to worsening the indoor thermal conditions in buildings while also increasing the energy demand for cooling [4]. This is a crucial issue in the Mediterranean countries where environmental phenomena such as heat waves will be more frequent in the next years [5]. Therefore, the main challenge that dominates the energy and environmental policies of most countries is to decarbonize the building sector through the reduction of its energy consumptions, and to improve the outdoor microclimate at urban scale [6, 7, 8]. To achieve these goals, several studies have investigated the effectiveness of vegetated-based strategies such as green roofs and vertical greening systems [9, 10]. These strategies can mitigate the urban microclimate contributing to improve the outdoor thermal comfort and reduce the cooling energy demand in buildings thanks to the evapotranspiration phenomena and shading effect of the plants [9, 11]. Although the traditional green roofs have several thermal and environmental benefits, they show some limitations such as the variation of the thermophysical properties of the growing substrate with the water content of the soil layer, remarkably affecting the energy balance of the green roof [12].

In this last decade, Building Integrated Architecture (BIA) is established as an interesting strategy to reduce energy consumption and realize urban sustainability by integrating soil-less plant cultivations within the buildings to promote urban food production while, optimizing nutrient management of the plants [13]. In this context, the hydroponic roof represents an alternative solution to the traditional green roof, providing several benefits such as reduction of land exploitation and efficient water use, reduction in air pollution, increase in food production, and reduction of maintenance costs with respect to the green roof systems [14]. Among different types of hydroponic cultivations, the Deep-Water culture (DWC) system is the most popular choice, particularly suitable for building applications, for quickly and efficiently growing many types of plants from edible species, herbs to various ornamental plants [15]. In DWC system, the plants grow with their roots submerged in a nutrient-rich and oxygenated water solution; the water depth has values up to 50 cm, providing greater stability of the nutrient solution and a fundamental action of thermal regulation compared to other hydroponic cultivation types [16]. However, water depths below 15–20 cm may adversely affect plant development by restricting proper root growth and function. The water volume acts as thermal buffer, stabilizing water temperature fluctuations caused by day-night cycles and serving as a thermal insulation layer for buildings [17]. This latter reveals the key role of the water layer affecting the energy performance and thermal behavior of the hydroponic roof.

Only few studies have adopted numerical modelling to investigate the energy performance of hydroponic roofs [15]. In this context, Ibrahim et al. [18], adopting a simulation approach for a hydroponic roof with 15 cm-deep water layer in Alexandria (Egypt), obtained reductions of 14% in cooling and 10% in heating energy needs compared to a bare roof. However, there is a lack of studies concerning the thermal behavior in transient regime of the hydroponic roofs to assess how the water layer affects the energy needs for space cooling, and the thermal inertia of the roof.

The present study aims to estimate the energy demand and assess the thermal dynamic behavior of a roof in presence of a DWC hydroponic module, by varying the depth of the water tray in three different roof typologies. To this aim, a validated dynamic TRNSYS model has been built for a modular DWC hydroponic roof prototype installed at University of Catania and designed within the Italian PRIN research project FUD-OF-SITHY (“*Favor the Urban Development OF Sustainable agriculture Through Hydroponics*”). The purpose of this work is to refine the hydroponic roof module in order to find a good compromise between technological solution and optimization of energy and thermal performance.

2 Materials and Methods

2.1 Description of the DWC hydroponic module prototype

The DWC hydroponic module prototype was installed on the flat roof of an existing building of the Civil Engineering and Architecture Department, at University Campus in Catania, a city in southern Italy located along the Mediterranean coast, characterized by warm and humid summer and moderately cool and wet winters. The installation site is a three-story reinforced concrete building with roof realized with reinforced concrete slab and hollow clay blocks, covered with concrete tiles.

Figure 1a shows the aerial view of the building where the experimental set-up is placed. Figure 1b and Figure 1c depict the experimental set-up of the hydroponic module while Figure 1d shows the materials used in the DWC hydroponic system.

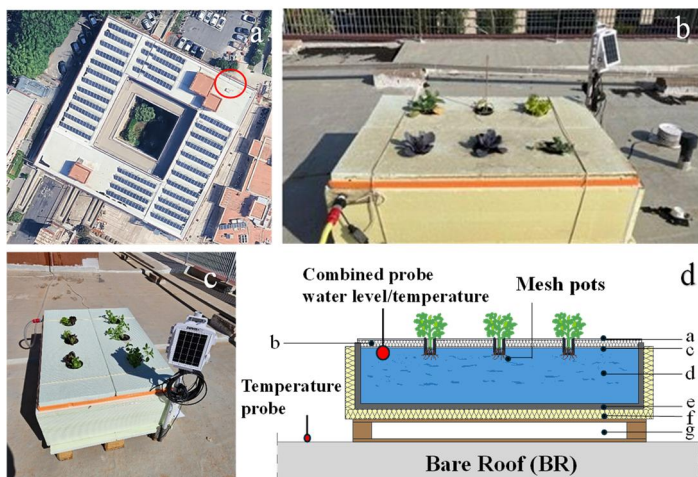


Fig. 1. Prototype of DWC hydroponic module: a) Placement of experimental set-up; b) and c) Experimental set-up; d) Stratigraphy and material used.

The experimental apparatus is based on the DWC system, where the plants are placed in a perforated polystyrene board that keeps them on top of a tray filled with a solution based on water and nutrients, where the roots are submerged. A water layer depth greater than 15 cm was selected to prevent potential root growth limitations in hydroponic crops. The growth bed is made with a 100 cm × 100 cm plastic tank, volume of 240 liters, height of 35 cm, filled with 30 cm of water. The plastic tank is thermally insulated with a layer of extruded polystyrene (XPS) with a thickness of 5 cm on the vertical sides and the bottom respectively. The opaque top lid shell covers the water tank reducing the daily evaporation and algae

growth. Two experimental hydroponic cultivations have been tested simultaneously such as lettuce (*Lactuca sativa*) and basil (*Ocimum basilicum*), chosen because of their reduced growth period and high adaptability to hydroponic systems. The thermo-physical features of the layers (a-g) of the DWC hydroponic module (HR) are reported in Table 1.

Table 1. Layers and thermal features of the hydroponic module.

	Layers	t [cm]	λ [W/(m·K)]	ρ [kg/m ³]	c_p [J/(kg·K)]
a	Polycarbonate top lid shell	1.0	0.20	1200	1200
b	Extruded polystyrene (XPS)	3.0	0.032	33	1450
c	Polycarbonate bottom lid shell	1.0	0.20	1200	1200
d	Water solution	30.0	0.56	1000	4186
e	Polycarbonate floor	3.0	0.20	1200	1200
f	Extruded polystyrene (XPS)	5.0	0.032	33	1450
g	Slightly ventilated air gap	4.0	0.20	1.2	1000

More information and details about the thermal features of the Hydroponic roof can be found in [19]. The DWC system is also equipped with a recirculation pump, and a water reintegration system to ensure continuous water circulation and homogenized distribution of the nutrients. Additionally, an oxygenator provides an optimum oxygen supply for the plant’s roots. The experimental set-up includes a fixed wireless weather station to detect the weather data used to calibrate the simulation model, and wireless node equipped with probes to collect the external surface temperature of the existing bare roof and the water temperature inside the tray of hydroponic module used to validate the TRNSYS simulation model. The measurements campaign was conducted over a six-month period, across the hottest summer months in Catania (from 25th June 2024 to 25th October 2024). Please check [19], for further details.

2.2 TRNSYS simulation model

The modelling of the DWC hydroponic module was carried out in dynamic thermal regime using TRNSYS software. To this aim, a sample room with intended office use has been modelled in the “Multi-zone building model” (Type 56). The room has a gross volume of 24.3 m³, a gross height of 2.70 m and a net floor area of 9.0 m². All walls adjacent to other rooms have been assumed to be adiabatic surfaces, except for the south-facing wall that has a window with surface of 1.2 m². The external wall is made of alveolate clay blocks without thermal insulation ($U_{wall} = 0.50$ W/(m²·K)), the roof is an uninsulated flat reinforced concrete slab with hollow clay blocks ($U_{roof} = 1.57$ W/(m²·K)), while the window is a common double-glazing with air gap ($U_{window} = 2.80$ W/(m²·K)). The solar absorptivity (α_{os}) and thermal emissivity (ϵ_{os}) of the outermost roof surface are 0.7 and 0.9, respectively. The air infiltration rate is set at a constant value of 0.5 ACH throughout the day, while internal gains follow a typical office schedule characterized by a use profile from 8:00 to 18:00 during workdays with a density of 0.1 people/m². The power density of equipment and lighting is set to 6 W/m² and 4 W/m² respectively.

The hydroponic module has been modelled by modifying the parameters of the green roof component (Type 785), as already suggested by [20], and then coupling this component with

the Type 56 (“multi-zone building model”). In particular, the soil layer has been treated as a homogeneous water layer with a water content of 100% during the entire simulation period. This assumption accounts for the continuous water replenishment to guarantee that the small amount of water lost due to evaporation does not alter the system’s thermal performance. For the vegetation layer, the radiative properties (α_{veg} and ϵ_{veg}) of the leaves have been taken from [21], while its fraction (X_{veg}) has been determined considering the horizontal projected area of the leaves under full development. For the detailed phases regarding the modelling of the hydroponic roof in TRNSYS and the calibration of the simulation model see [22]. All the input parameters adopted for modelling the hydroponic module in TRNSYS are reported in Table 2.

Table 2. Input parameters required by TRNSYS Type 785 for modelling the DWC Hydroponic module.

Parameters	Name	Unit	Value
Vegetation fraction	X_{veg}	ND	0.15
Vegetation absorptivity	α_{veg}	ND	0.60
Vegetation emissivity	ϵ_{veg}	ND	0.97
Solar absorptivity of the top lid	α_{os}	ND	0.40
Emissivity of the top lid	ϵ_{os}	ND	0.90
Area of water tray	A_w	m ²	1.00
Thermal conductivity of water	λ_w	W/(m K)	0.60
Density of water	ρ_w	kg/m ³	1000
Specific heat of water	$c_{p,w}$	J/(kg K)	4186
Bare roof U-value	U_{BR}	W/(m ² K)	1.57
Water content	$\Theta_{w,i}$	ND	100%
Initial water temperature	$T_{w,i}$	°C	14.8

Regarding the treatment of evaporative effects, Type 785 inherently accounts for evapotranspiration effects at the vegetation-atmosphere interface through the energy balance of the canopy layer. However, in the present modelling approach, the water layer is treated as fully covered by the opaque polycarbonate lid, which substantially limits direct evaporation from the water surface. The model assumes that the small evaporative losses occurring through the openings for the plants are continuously compensated by the water replenishment system, maintaining constant water content throughout the simulation period. This assumption is consistent with the experimental conditions, where daily evaporation was found to be negligible (less than 2 mm/day). Consequently, evaporative cooling from the water surface plays a minor role in the overall thermal balance, compared with the water thermal inertia and the radiative exchange at the top lid surface.

An on-site experimental measurement campaign allowed detecting the external surface temperature on the existing bare roof (BR) and the water temperature in the hydroponic tray (HR) during a six-month period to validate the simulation model. The statistical indexes based on the detailed investigation of the hourly profiles of temperature measured on the outer side of bare roof and in the water tray of hydroponic module against those predicted through TRNSYS showed good agreement: MAE < 0.40°C and coefficient of determination $R^2 = 0.90$ for Hydroponic module (HR), while MAE = 2.30 °C and $R^2 = 0.91$ for bare roof (BR) [22]. Thereby, the model was considered validated for carrying out the roof configuration analysis described hereafter.

Based on the validated thermal model, the annual simulations of the office room were carried out by using thermostatic control switched on during workdays (from 8:00 to 18:00) to calculate the seasonal energy demand for heating and cooling under different selected roof configurations. The energy demand for space heating (HEd) has been calculated from 1st December to 31st March using a set-point temperature of 20 °C, while the energy demand for space cooling (CEd) has been calculated from 1st June to 30th September with a set-point temperature of 26 °C according to the standard regulation of climate zone of Catania. Moreover, annual free-running simulations were performed to investigate the dynamic thermal behaviour of the selected hydroponic roof configurations. The surface temperature on the outer surface (T_{os}) and inner surface (T_{is}) of the roof was analysed in detail during a typical hot summer week (9th to 16th July). Dynamic thermal parameters such as the Time Lag (TL) and the Decrement Factor (DF) were calculated for all the roof scenarios in relation to the inner and the outer surface temperatures of the roof, based on the results of hourly simulations in free-running conditions.

2.3 Investigated roof configurations

Figure 2 reports all the roof typologies investigated (*HB*, *INS HB*, *LW*) under bare configurations and in presence of a hydroponic module with water depth of the tray variable from 20 cm to 40 cm.

Uninsulated concrete roof		Insulated concrete roof		Prefabricated Lightweight roof	
	HB		INS_HB		LW
	HB_HR_I		INS_HB_HR_I		LW_HR_I
	tw = 20 cm		tw = 20 cm		tw = 20 cm
	HB_HR_II		INS_HB_HR_II		LW_HR_II
	tw = 30 cm		tw = 30 cm		tw = 30 cm
	HB_HR_III		INS_HB_HR_III		LW_HR_III
	tw = 40 cm		tw = 40 cm		tw = 40 cm

Fig. 2. Investigated roof scenarios.

The stratigraphy, and the thermophysical features of the layers of the investigated roof typologies *HB*, *INS_HB*, and *LW* are reported in Table 3. Table 4 reports the thicknesses (t), the U-value, and the surface mass (SM) of the investigated roof scenarios. Each scenario was defined by maintaining the features reported in Table 3 and just varying for each typology of roof (e.g., *HB*, *INS_HB*, and *LW*) the water depth inside the tray (t_w).

Table 3. Layers and thermal features of the *HB*, *INS_HB*, *LW* configurations.

Scenarios	Layer	t [cm]	λ [W/(m·K)]	ρ [kg/m ³]	cp [J/(kg·K)]
HB	Clay tiles	2.0	1.50	1500	1000
	Lightweight concrete	4.0	1.00	1400	1200
	Waterproofing membrane	0.2	0.20	1000	1200
	Hollow clay blocks + concrete slab	22.0	0.56	1280	1000
	Lime and cement mortar	3.0	0.90	1000	1000
	INS_HB	Clay tiles	2.0	1.50	1500
INS_HB	Lightweight concrete	4.0	1.00	1400	1200
	Waterproofing membrane	0.2	0.20	1000	1200
	Extruded polystyrene layer	8.0	0.034	15	1450
	Bitumen layer	0.2	0.17	1200	1000
	Hollow clay blocks + concrete slab	22.0	0.56	1280	1000
	Lime and cement mortar	3.0	0.90	1000	1000
LW	Oriented Strand Board (OSB)	0.9	0.12	650	1700
	Polystyrene layer	6.5	0.04	15	1450
	Oriented Strand Board (OSB)	0.6	0.12	650	1700

Table 4. Main thermal features of the investigated roof scenarios.

Investigated roof typology	t _w [cm]	Roof configurations	t _r [cm]	U [W/(m ² ·K)]	SM [kg/m ²]
HB	0	HB	32	1.57	367
	20	HB_HR_I	64	0.27	576
	30	HB_HR_II	74	0.26	671
	40	HB_HR_III	84	0.25	722
INS_HB	0	INS_HB	40	0.34	422
	20	INS_HB_HR_I	72	0.16	602
	30	INS_HB_HR_II	82	0.15	705
	40	INS_HB_HR_III	92	0.14	780
LW	0	LW	8	0.52	15
	20	LW_HR_I	40	0.20	213
	30	LW_HR_II	50	0.195	313
	40	LW_HR_III	60	0.19	413

3 Results and discussions

3.1 Seasonal energy demand

The thermal energy demand and the corresponding energy savings for heating (HEd) and cooling (CEd) for each investigated roof typology (*HB*, *INS_HB*, *LW*) in the bare

configurations and in presence of hydroponic module (*HR*) with different depth values of water in the tray (I: $t_w = 20$ cm; II: $t_w = 30$ cm; III: $t_w = 40$ cm) are reported in Figure 3 (a-b) and in Table 5.

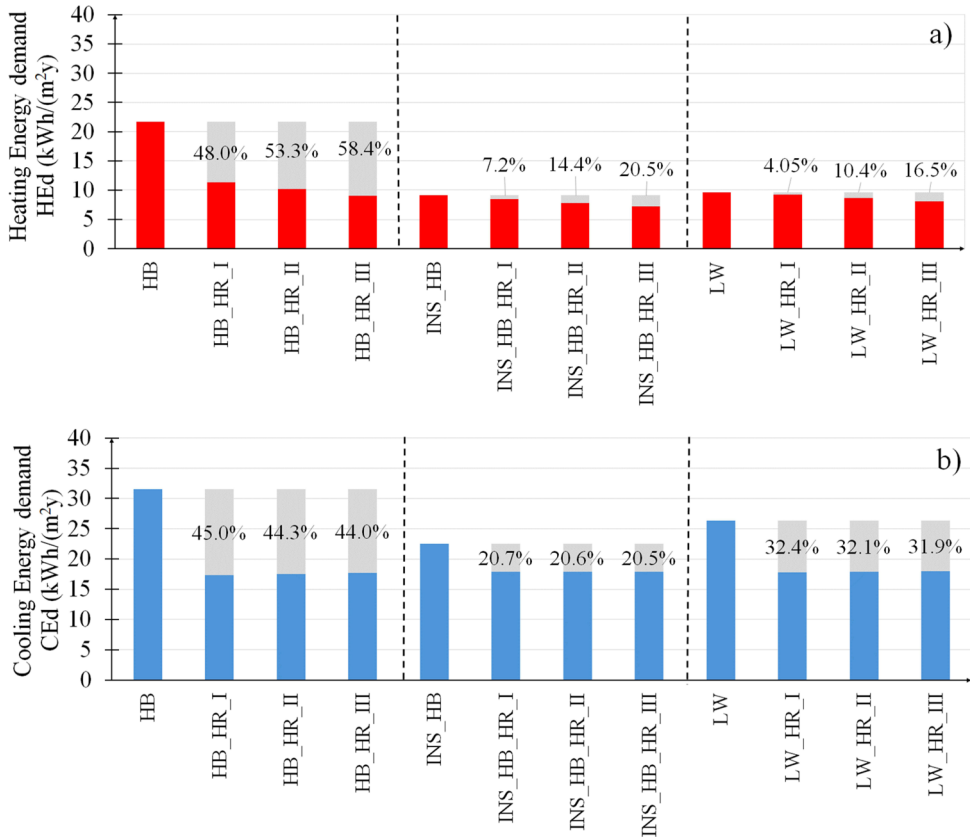


Fig. 3. Thermal energy needs per unit of net floor area: a) Heating; b) Cooling.

The uninsulated concrete roof with clay blocks (*HB*) is characterized by the highest energy demand for heating ($HEd = 21.71$ kWh/(m² y)) and cooling ($CEd = 31.53$ kWh/(m² y)), while the insulated roof configuration (*INS_HB*) requires the lowest energy demand ($HEd = 9.13$ kWh/(m² y), $CEd = 22.56$ kWh/(m² y)). The results revealed that the addition of a DWC hydroponic module with a depth of the water tray of 20 cm produced the highest reduction of the heating and cooling energy demand in all the investigated roof typologies in comparison with their bare configurations (*HB*, *INS_HB*, *LW*). In particular, the uninsulated concrete slab configuration (*HB_HR_I*) showed energy savings of around 48% for heating and 45% for cooling, respectively. However, a notable reduction in the cooling energy demand ($CE_s = 32\%$) can also be achieved in the lightweight prefabricated roof when a DWC hydroponic module is added.

Table 5. Seasonal energy demand for heating and cooling, and energy savings.

Roof typology	t_w [cm]	Configuration	HEd [kWh/(m ² ·y)]	HEs [%]	CEd [kWh/(m ² ·y)]	CEs [%]
HB	0	HB	21.71	–	31.53	–
	20	HB_HR_I	11.29	48.0	17.34	45.0
	30	HB_HR_II	10.14	53.2	17.54	44.3
	40	HB_HR_III	9.03	58.4	17.65	44.0
INS_HB	0	INS_HB	9.13	–	22.56	–
	20	INS_HB_HR_I	8.47	7.2	17.90	20.7
	30	INS_HB_HR_II	7.82	14.4	17.92	20.6
	40	INS_HB_HR_III	7.26	20.5	17.93	20.5
LW	0	LW	9.62	–	26.37	–
	20	LW_HR_I	9.23	4.1	17.82	32.4
	30	LW_HR_II	8.62	10.4	17.90	32.1
	40	LW_HR_III	8.03	16.5	17.95	31.9

Further increase of the water depth in the hydroponic tray contributed to the increase in the thermal resistance of the roof, thus involving a further reduction in the heating energy demand (HEd) by about 6%, while no appreciable improvement was observed in the cooling performance (see Figure 3). It should be noted that an increase of the water depth produced an increase in the cooling energy demand (CEd) for all investigated roof scenarios. This result is due to the increased thermal resistance of the roof, which reduces the heat loss from the indoor to the external environment.

3.2 Thermal dynamic behavior of the roof

Figure 4 shows the maximum values of surface temperature respectively on the outermost side and inner side of the roof ($T_{os,max}$; $T_{is,max}$), Time Lag (TL), and Decrement Factor (DF) for each investigated roof configuration related to a typical hot summer week (9th to 16th July). Table 6 reports the numerical values of the surface temperature ($T_{os,max}$; $T_{is,max}$), and dynamic thermal parameters (TL, DF).

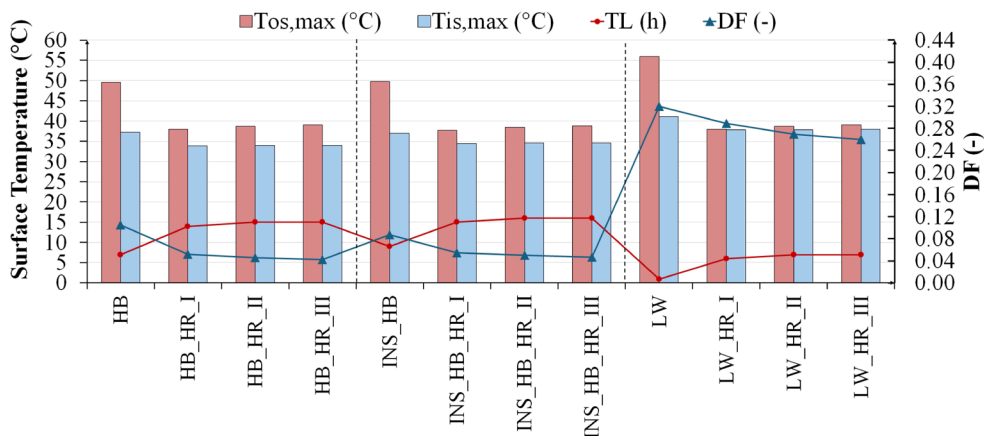


Fig. 4. Surface temperature and thermal dynamic properties for all the investigated roof scenarios.

Table 6. Surface temperatures, and thermal dynamic parameters for each investigated roof scenario.

Roof typology	t_w [cm]	Configuration	$T_{os,max}$ [°C]	$T_{is,max}$ [°C]	DF [-]	TL [h]
HB	0	HB	49.5	37.2	0.105	7
	20	HB_HR_I	38.0	33.9	0.052	14
	30	HB_HR_II	38.7	34.0	0.046	15
	40	HB_HR_III	39.0	34.0	0.042	15
INS_HB	0	INS_HB	49.8	37.0	0.087	9
	20	INS_HB_HR_I	37.7	34.5	0.055	15
	30	INS_HB_HR_II	38.4	34.6	0.050	16
	40	INS_HB_HR_III	38.8	34.6	0.047	16
LW	0	LW	56.0	41.1	0.321	0
	20	LW_HR_I	38.0	37.8	0.289	6
	30	LW_HR_II	38.7	37.9	0.271	7
	40	LW_HR_III	39.1	38.0	0.262	7

All the bare roof configurations (*HB*, *INS_HB*, *LW*) have a maximum value of outermost surface temperature ($T_{os,max}$) higher than 45°C, and peak values of the surface temperature on the inner side of the roof higher than 37°C. In particular, the prefabricated lightweight roof configuration (*LW*) has the highest peak values of T_{os} and T_{is} showing the poor values of the dynamic thermal properties. Indeed, the highest value of DF is detected for *LW* configuration which cannot allow to dampen the amplitude of the incoming heat flux and delay its peak value. On the contrary, the insulated lightweight concrete roof with hollow clay block (*INS_HB* configuration) showed a better thermal dynamic behavior (DF = 0.087; TL = 9 h) than other bare roof configurations.

It can be observed that the addition of a DWC hydroponic module with a water depth of 20 cm has provided a relevant improvement in the thermal behavior of all investigated roof typologies.

Looking at the peak values of the surface temperature of the roof, it can be noted that a decrease higher than 2.5 °C for $T_{is,max}$ in the (*HB_HR_I*, *INS_HB_HR_I*) configurations has been achieved. In addition, a hydroponic module is capable to provide a reduction higher than 10 °C in $T_{os,max}$ for all investigated roof scenarios with consequent benefits on the outdoor microclimate.

In presence of a DWC hydroponic module, the uninsulated lightweight concrete roof with hollow clay blocks (*HB_HR_I*) has provided the best dynamic thermal responses because TL increased from 7 h to 14 h and the amplitude of the fluctuation of incoming heat flux through the roof is notably dampened (DF is decreased from 0.108 to 0.052). It is worth highlighting that a further increase in the water depth of the tray did not provide any significant improvement both on surface temperatures and thermal dynamic parameters. On the contrary, an increase in the water depth of the tray slightly worsened the effects on the outdoor environment due to the higher values of $T_{os,max}$.

From a physical standpoint, the observed improvements in time lag (TL) and decrement factor (DF) can be directly related to the distribution of thermal mass and resistance within the roof assembly. The time lag is primarily governed by the product of thermal resistance (R) and heat capacity (C) of the layers encountered by the thermal wave. By adding the DWC

module, a significant amount of thermal mass (200 kg/m^2 for $t_w = 20 \text{ cm}$) is introduced at the outermost position of the roof, where it effectively intercepts and absorbs the incoming solar heat flux before it penetrates the underlying structure. The water layer, with its high specific heat capacity, acts as a thermal buffer that delays the peak heat flux transmission to the interior. This explains the doubling of the time lag from 7 h to 14 h observed in the *HB* configuration. The decrement factor, which represents the ratio between the amplitude of temperature oscillations at the inner and outer surfaces, is reduced because the thermal mass attenuates the magnitude of the heat wave as it propagates inwards. Notably, placing the high thermal mass externally, rather than internally, maximizes its effectiveness in damping external temperature fluctuations before they reach the building interior. For the lightweight roof (*LW*), which inherently lacks thermal mass ($SM = 15 \text{ kg/m}^2$), the addition of the water layer compensates for this deficiency, reducing the DF from 0.321 to 0.289 and introducing a time lag where none existed previously. Conversely, further increases in water depth (30–40 cm) yield diminishing returns because the additional thermal resistance impedes nocturnal radiative cooling, partially offsetting the benefits of increased thermal mass.

3.3 Discussion

The hydroponic module configuration with the tray depth of 20 cm is the best solution in all the investigated roof typologies because it provides the real breakthrough both in terms of energy demand for space cooling and dynamic thermal behaviour of the roof. The increase of the tray depth up to 30 or 40 cm does not lead to appreciable thermal benefits while slightly worsening the summer performances because the thermal mass of the roof tends to remain warm in the hottest hours. In addition, the surface temperature on the inner side of the roof is almost the same with the variation of the water depth from 20 cm to 40 cm for each investigated roof typology (*HB*, *INS_HB*, *LW*). This means that increasing the depth of the tray in a hydroponic roof configuration does not lead to real benefits for indoor thermal conditions. The surface temperature on the outermost layer of the hydroponic roof configuration slightly worsens with increasing water depth in all investigated roof typologies. Indeed, the outer surface temperature tends to increase when varying the tray depth from 20 to 40 cm: the increase of the peak value of outer surface temperature has impact on the outdoor microclimate conditions by contributing to the Urban Heat Island phenomenon.

As regards the effects of the hydroponic module on the thermal behaviour of the various roof typologies, it is worth observing that the lightweight prefabricated roof (*LW*) shows overall a pronounced improvement when a hydroponic tray depth of 20 cm is added. Indeed, a percentage saving of 32% in the cooling energy demand, and a reduction of the decrement factor with an increase of the time lag, can be obtained in *LW_HR_I* configuration. In addition, this configuration shows the maximum reduction in the surface temperature on the outermost layer of the roof that is crucial for mitigating the impact Urban Heat Island effect. On the contrary, the addition of a water tray with depth of 20 cm marginally improves the energy performance and thermal behaviour of the insulated concrete roof (*INS_HB*) because this roof configuration shows overall a good performance in its bare configuration.

The uninsulated concrete roof (*HB*) shows the worst energy performance in the bare configuration while it is the best configuration when a tray with water depth of 20 cm is added. Indeed, the highest energy savings in the heating and cooling energy demand in the *HB_HR_I* configuration are obtained ($HE_s = 48\%$; $CE_s = 45\%$). Under free-running conditions, a maximum reduction in the peak value of surface temperature on the inner side of the roof is achieved with consequent improvement of the indoor thermal conditions. In addition, the configuration (*HB_HR_I*) allows to obtain the maximum reduction of the decrement factor and the maximum increase in the time lag of the peak of incoming heat flux through the roof involving a good thermal dynamic behaviour of the roof. It should be

acknowledged that the DWC hydroponic system requires additional operational energy inputs that are not accounted for in the present thermal analysis. These include the electricity consumption of the recirculation pump and the oxygenator, which are essential to maintain adequate nutrient circulation and root oxygenation. Although such energy requirements are generally modest compared to the space conditioning loads, i.e. typically in the range of 5–15 W per module for continuous operation, their contribution to the overall energy balance should be considered in a comprehensive life-cycle assessment. Future work will address a detailed energy audit of the ancillary components to provide a complete picture of the net energy benefits of the system.

4 CONCLUSIONS

This study evaluated the energy performance and thermal dynamic behavior of roofs equipped with a Deep Water Culture (DWC) hydroponic module through validated transient simulations. The analysis focused on the effect of varying the water depth of the hydroponic tray (20, 30 and 40 cm) when applied to three representative roof typologies: uninsulated concrete slabs with hollow clay blocks, insulated concrete roofs and lightweight prefabricated roofs. The results clearly indicate that a hydroponic tray depth of 20 cm constitutes the optimal solution for all investigated configurations. At this depth, the DWC module provides a balanced combination of thermal inertia and thermal resistance, leading to substantial reductions in cooling energy demand, significant attenuation and delay of heat flux transmission and marked decreases in peak external and internal surface temperatures. These effects are particularly pronounced in lightweight roof systems, where the added thermal mass effectively compensates for the lack of inherent inertia, yielding cooling energy savings of up to 32% and a notable improvement in thermal dynamic performance.

Conversely, increasing the water depth to 30 cm and 40 cm does not result in further energy or thermal benefits. On the contrary, excessive water depth increases the overall thermal resistance of the roof, limiting nocturnal heat dissipation and promoting heat accumulation during summer conditions. This phenomenon leads to marginally higher internal surface temperatures and a slight increase in cooling energy demand, as well as higher external surface temperatures that may negatively affect the urban microclimate.

The insulated concrete roof exhibits comparatively smaller improvements when equipped with the hydroponic module, as its bare configuration already provides good thermal performance. This outcome confirms that the effectiveness of hydroponic roofs is strongly dependent on the initial thermal characteristics of the building envelope.

In conclusion, DWC hydroponic roofs represent a promising passive solution for building retrofitting, particularly in warm climates and for lightweight or poorly insulated roofs. Their effectiveness, however, is not proportional to the amount of water used: beyond a critical threshold, increasing the water depth becomes counterproductive. Future research should therefore focus on a more detailed seasonal energy balance and heat-flux analysis, as well as on the influence of additional parameters such as variable water levels, alternative insulation materials for the tray and different plant coverage ratios, to further optimize the design and applicability of hydroponic roof systems.

Nomenclature

- CEd* Cooling energy demand, kWh/(m² y)
CEs Cooling energy saving, %
c_p Specific heat, J/(kg K)
DF Decrement Factor, ND
HEd Heating energy demand, kWh/(m² y)
HEs Heating energy saving, %
MAE Mean Absolute Error, °C
R² Coefficient of determination
SM Surface Mass, kg/m²
t Thickness, cm
t_r Roof thickness, cm
t_w Depth of the hydroponic tray, cm
T_{is} Inner surface temperature, °C
T_{os} Outer surface temperature, °C
TL Time Lag, h
U Thermal transmittance, W/(m² K)
X_{veg} Fraction of roof surface covered by the vegetation, ND
- Greek symbols*
α Solar absorptivity, ND
ε Thermal emissivity, ND
Θ Water content, ND
λ Thermal conductivity, W/(m K)
ρ Density, kg/m³

This research was made possible through the generous support of the FUD-OF-SITHY project – “Favor the Urban Development OF Sustainable Agriculture Through HYdroponics” – P2022F9HEW, funded under the National Recovery and Resilience Plan (PNRR) with the identifier CUP E53D23017150001, and of the PIA.CE.RI. 2024-2026 Linea 1 GREEN project (PI prof. F. Nocera).

References

1. UN, About the sustainable development goals 2019 (New York, 2019)
2. S. Chapman, J.-E.-M. Watson, A. Salazar, M. Thatcher, C.A. McAlpine, The impact of urbanization and climate change on urban temperatures: a systematic review, *Landscape Ecol.* **32**(10), 1921–1935 (2017). <https://doi.org/10.1007/s10980-017-0561-4>
3. Y.H. Chen, J.T. Wu, K. Yu, Evaluating the impact of the building density and height on the block surface temperature. *Build. Environ.* **168**(1), 106493 (2020). <https://doi.org/10.1016/j.buildenv.2019.106493>
4. J. Paravantis, M. Santamouris, C. Cartalis, C. Efthymiou, N. Kontoulis, Mortality Associated with High Ambient Temperatures, Heatwaves, and the Urban Heat Island in Athens, Greece. *Sustainability* **9**, 606 (2017). <https://doi.org/10.3390/su9040606>
5. H.L. Macintyre, C. Heaviside, J. Taylor, R. Picetti, P. Symonds, X.M. Cai, S. Vardoulakis, Assessing urban population vulnerability and environmental risks across an urban area during heatwaves. *Sci. Total Environ.* **610**, 678–690 (2018). <https://doi.org/10.1016/j.scitotenv.2017.08.062>

6. K. Szulecki, D.H. Claes, Towards Decarbonization: Understanding EU Energy Governance. *Polit. Govern.* **7**(1), 1–5 (2019). <https://doi:10.17645/pag.v7i1.2029>
7. A. Gagliano, F. Nocera, G. Tina, Performances and economic analysis of small photovoltaic–electricity energy storage system for residential applications. *Energy Environ.* **31**(1), 155 – 175 (2020). <https://doi:10.1177/0958305X18787313>
8. F. Nocera, R. Caponetto, G. Giuffrida, M. Detommaso, Energetic retrofit strategies for traditional sicilian wine cellars: A case study. *Energies* **13**(12), 3237 (2020). <https://doi:10.3390/en13123237>
9. J. Dong, M. Lin, T. Zuo, J. Liu, C. Sun, J. Luo, Quantitative study on the cooling effect of green roofs in a high-density urban area—A case study of Xiamen, China. *J. Clean. Prod.* **255**, 120–152 (2020). <https://doi.org/10.1016/j.jclepro.2020.120152>
10. M. Detommaso, V. Costanzo, F. Nocera, G. Evola, Evaluation of the cooling potential of a vertical greenery system coupled to a building through an experimentally transient model. *Build. Environ.* **244**, 110769 (2023). <https://doi.org/10.1016/j.buildenv.2023.110769>
11. G. Pérez, J. Coma, M. Chàfer, L.F. Cabeza, Seasonal influence of leaf area index (LAI) on the energy performance of a green façade. *Build. Environ.* **207**, Part B, 108497 (2022). <https://doi.org/10.1016/j.buildenv.2021.108497>
12. D.J. Sailor, D. Hutchinson, L. Bokovoy, Thermal property measurements for ecoroof soils common in the western U.S. *Energy Build.* **40**, 1246–1251 (2008). <https://doi:10.1016/j.enbuild.2007.11.004>
13. J. Muñoz-Liesa, S. Toboso-Chavero, A. Mendoza Beltran, E. Cuerva, E. Gallo, S. Gassó-Domingo, A. Josa, Building-integrated agriculture: Are we shifting environmental impacts? An environmental assessment and structural improvement of urban greenhouses. *Resour. Conserv. Recycl.* **169**, 105526 (2021). <https://doi.org/10.1016/j.resconrec.2021.105526>
14. N. Sabeh, Rooftop plant production systems in urban areas, *Plant Factory, An Indoor Vertical Farming System for Efficient Quality Food Production*, 129–135 (Academic Press, 2020). <https://doi.org/10.1016/B978-0-12-816691-8.00007-8>
15. R. Rapisarda, F. Nocera, V. Costanzo, G. Sciuto, R. Caponetto, Hydroponic green roof systems as an alternative to traditional pond and green roofs: a literature review. *Energies* **15**, 2190 (2022). <https://doi.org/10.3390/en15062190>
16. M. Majid, J.N. Khan, Q.M.A. Shah, K.Z. Masoodi, B. Afroza, S. Parvaze, Evaluation of hydroponic systems for the cultivation of Lettuce. *Agric. Water Manag.* **245**, 106572 (2021). <https://doi:10.1016/j.agwat.2020.106572>
17. J.E. Son, H.J. Kim, T.I. Ahn, Hydroponic systems, *Plant Factory, An Indoor Vertical Farming System for Efficient Quality Food Production*, 273–283 (Academic Press, 2020). <https://doi.org/10.1016/B978-0-12-816691-8.00020-0>
18. A.M. Ibrahim, W.F. Omar, M.A. Mahdy, The Effect of Hydroponics Planted Roof on the Thermal Performance of Indoor Residential Spaces in Egypt. *Sci. J. Fac. Fine Arts* **10**(2) (2022).
19. F. Nocera, V. Costanzo, G. Evola, M. Detommaso, A. Gagliano, M. Cellura, M. Mistretta, S. Longo, Cooling buildings and growing food: performance evaluation of a hydroponic roof system in a Mediterranean climate, in *Proceedings of the Cisbat 2025, The built environment in transition, Hybrid International Scientific Conference, Lausanne, Switzerland, September 3-5 (2025)*.

20. J. Hong, Optimal design of green roofs: Mathematical model and experimental evidence, Ph.D. thesis, University of Wisconsin-Milwaukee (2018)
21. D.M. Gates, Biophysical ecology (Dover Publications, New York, 2003)
22. F. Nocera, V. Costanzo, G. Evola, M. Detommaso, M. Cellura, M. Mistretta, S. Longo, Experimental Validation and TRNSYS Modeling of a Modular Hydroponic Roof System for Thermal Performance Assessment, in Proceedings of 17th KES International Conference on Sustainability in Energy and Buildings, Catania, Italy, September 17-19 (2025)